Ultrafast Electrosynthesis of High Hydrophobic Polypyrrole Coatings on a Zinc Electrode: Applications to the Protection against Corrosion

Eric Hermelin,[†] Jacques Petitjean,[†,‡] Jean-Christophe Lacroix,[†] Kathleen Isabelle Chane-Ching,[†] Jean Tanguy,[†] and Pierre-Camille Lacaze*[,†]

Interfaces, Traitements, Organisation et Dynamique des Systèmes (ITODYS), Université Paris 7-Denis Diderot, CNRS, UMR 7086, 1 rue Guy de la Brosse, 75005 Paris, France, and LEDEPP, USINOR Recherche et Développement, Florange, France

Received December 21, 2007. Accepted March 31, 2008

Hydrophobic polypyrrole (PPy) coatings on zinc electrodes were prepared by a one-step electrochemical method. The process is ultrafast; 2 μm of PPy can be deposited in less than 3 s. It is thus compatible with industrial requirements for the coating of large surfaces for various industries (automotive, buildings, ships). The coatings obtained have apparent contact angles as high as 125° and can thus be used as cheap highly hydrophobic surfaces. They have been fully characterized using various physicochemical techniques (EQCM, XPS) and their anticorrosion properties have been tested. It is found that postpolymerization heat treatment makes it possible to reach a situation where 1 μm of polypyrrole is equivalent to 1 μm of a zinc coating for preventing the corrosion of mild steel.

1. Introduction

Conductive polymers have been proposed as anticorrosion layers. Our group,[1–6] among many others,[7–30] is involved in this research field. In a previous paper,[31] we showed how sodium salicylate could be used as an electrolyte for depositing polypyrrole (PPy) films on oxidizable metals such as zinc by the electrochemical oxidation of pyrrole. In spite of the very large gap between the pyrrole and zinc oxidation potentials, which thermodynamically should lead to metal dissolution and not to polymer formation, PPy films were formed as easily as on a platinum electrode. This surprising result is explained by the fact that a very thin, passivating, composite zinc salicylate layer ($ZnSac_2$), formed prior to pyrrole electropolymerization, prevents zinc dissolution without inhibiting polymer formation. It was found that this passivation layer was very thin (around 15 nm) and did not desorb at the pyrrole oxidation potential. The ultrafast electropolymerization of pyrrole through this passivating layer was attributed to the presence of conductive pyrrolic paths inside the salicylate layer, which make this composite layer as active as a noble metal.[32]

One of the major applications of zinc is as a sacrificial anticorrosion layer for mild steel in diverse technological domains in the marine, automobile, aviation and building industries. Cheap, self-cleaning and anticorrosive properties of highly hydrophobic zinc surfaces are thus of interest. PPy has been recently proposed for smart surfaces with reversible switchable wettability,[33] and superhydrophobic surfaces have proved useful for the design of new anticorrosion layers. [34–38]

* Corresponding author. E-mail: lacaze@univ-paris-diderot.fr.
[†] Université Paris 7-Denis Diderot.
[‡] USINOR Recherche et Développement.

(1) Camalet, J. L.; Lacroix, J. C.; Aeiyach, S.; Ching, K. I. C.; Lacaze, P. C. *Synth. Met.* **1999**, *102* (1−3), 1386–1387.
(2) Camalet, J. L.; Lacroix, J. C.; Nguyen, T. D.; Aeiyach, S.; Pham, M. C.; Petitjean, J.; Lacaze, P. C. *J. Electroanal. Chem.* **2000**, *485* (1), 13–20.
(3) Nguyen, T. D.; Camalet, J. L.; Lacroix, J. C.; Aeiyach, S.; Pham, M. C.; Lacaze, P. C. *Synth. Met.* **1999**, *102* (1−3), 1388–1389.
(4) dos Santos, L. M. M.; Lacroix, J. C.; Chane-Ching, K. I.; Adenier, A.; Abrantes, L. M.; Lacaze, P. C. *J. Electroanal. Chem.* **2006**, *587* (1), 67–78.
(5) Meneguzzi, A.; Pham, M. C.; Lacroix, J. C.; Piro, B.; Adenier, A.; Ferreira, C. A.; Lacaze, P. C. *J. Electrochem. Soc.* **2001**, *148* (4), B121−B126.
(6) Meneguzzi, A.; Pham, M. C.; Ferreira, C. A.; Lacroix, J. C.; Aeiyach, S.; Lacaze, P. C. *Synth. Met.* **1999**, *102* (1−3), 1390–1391.
(7) Li, P.; Tan, T. C.; Lee, J. Y. *Synth. Met.* **1997**, *88* (3), 237–242.
(8) Santos, J. R.; Mattoso, L. H. C.; Motheo, A. J. *Electrochim. Acta* **1998**, *43* (3−4), 309–313.
(9) Bernard, M. C.; Hugot-LeGoff, A.; Joiret, S.; Dinh, N. N.; Toan, N. N. *J. Electrochem. Soc.* **1999**, *146* (3), 995–998.
(10) Kinlen, P. J.; Menon, V.; Ding, Y. W. *J. Electrochem. Soc.* **1999**, *146* (10), 3690–3695.
(11) Wessling, B.; Posdorfer, J. *Electrochim. Acta* **1999**, *44* (12), 2139–2147.
(12) Herrasti, P.; Ocon, P. *Appl. Surf. Sci.* **2001**, *172* (3−4), 276–284.
(13) Le, H. N. T.; Garcia, B.; Deslouis, C.; Le Xuan, Q. *Electrochim. Acta* **2001**, *46* (26−27), 4259–4272.
(14) Rajagopalan, R.; Iroh, J. O. *Electrochim. Acta* **2001**, *46* (16), 2443–2455.
(15) Roux, S.; Audebert, P.; Pagetti, J.; Roche, M. *J. Mater. Chem.* **2001**, *11* (12), 3360–3366.
(16) Bazzaoui, M.; Martins, L.; Bazzaoui, E. A.; Martins, J. I. *Electrochim. Acta* **2002**, *47* (18), 2953–2962.
(17) Fenelon, A. M.; Breslin, C. B. *Electrochim. Acta* **2002**, *47* (28), 4467–4476.
(18) Asan, A.; Kabasakaloglu, M. *Mater. Sci.* **2003**, *39* (5), 643–651.
(19) Tan, C. K.; Blackwood, D. J. *Corros. Sci.* **2003**, *45* (3), 545–557.
(20) Malik, M. A.; Wlodarczyk, R.; Kulesza, P. J.; Bala, H.; Miecznikowski, K. *Corros. Sci.* **2005**, *47* (3), 771–783.
(21) Pournaghi-Azar, M. H.; Nahalparvari, H. *Electrochim. Acta* **2005**, *50* (10), 2107–2115.
(22) Yagan, A.; Pekmez, N. O.; Yildiz, A. *J. Electroanal. Chem.* **2005**, *578* (2), 231–238.
(23) Bonastre, J.; Garces, P.; Huerta, F.; Quijada, C.; Andion, L. G.; Cases, F. *Corros. Sci.* **2006**, *48* (5), 1122–1136.
(24) Pawar, P.; Gaikawad, A. B.; Patil, P. P. *Sci. Technol. Adv. Mater.* **2006**, *7* (7), 732–744.
(25) Vatsalarani, J.; Geetha, S.; Trivedi, D. C.; Warrier, P. C. *J. Power Sources* **2006**, *158* (2), 1484–1489.
(26) Yano, J.; Nakatani, K.; Harima, Y.; Kitani, A. *Electrochemistry* **2006**, (11), 877–882.

10.1021/cm703658t CCC: $40.75 © 2008 American Chemical Society
Published on Web 06/04/2008

In this work, we study the effects of some structural variations of the salicylate anion on the general properties of the PPy films. A new electrolyte was selected for this study, 3,5-diisopropylsalicylic acid, which differs from salicylic acid in the presence of two large hydrophobic isopropyl groups attached to the phenyl ring, which could enhance the contact angle of the coating and influence the protection properties of the PPy films.

Experiments were carried out on stationary and stirred solutions. This latter case is important, because for industrial applications, in particular in the case of the zinc electroplating process, the steel plate to be zincated runs very quickly through the electrolysis bath (at about 1 m s^{-1}). The paint primer application follows under hydrodynamic conditions equivalent to those of a disk electrode rotating at a speed of about 2500 rpm.

2. Experimental Section

Polypyrrole films were prepared by electropolymerization of 0.5 M pyrrole (Acros 99%) in a sodium salicylate solution (Acros 99%) or in a mixture of sodium salicylate and 3,5-diisopropyl salicylic acid. All voltammetric experiments were performed in a standard single-compartment three-electrode cell connected to an EG&G PAR (Princeton Applied Research) model 273A potentiostat/galvanostat and driven by EG&G Power Suite software. The working electrode was a zinc disk (diameter 5 mm, Weber, >99.9%) mounted on a Radiometer EDI 101 and rotated by a Radiometer CTV 101. Prior to each experiment, the disk was polished with 1200-grade abrasive paper, degreased in acetone, rinsed in pure ethanol, and dried in air. The counter-electrode was a stainless steel plate and the reference electrode a Tacussel KCl saturated calomel (SCE). Unless stated otherwise, all experiments were performed at a polarization rate of 10 mV s^{-1}.

EQCM electrochemical measurements were performed in the potentiodynamic mode at 10 or 5 mV s^{-1}. The current was recorded simultaneously with the quartz frequency change as a function of potential. A platinum wire was used as a counter-electrode and the potential was referred to the saturated calomel electrode (SCE). The working electrode was an "AT-cut" quartz crystal oscillating at 9 MHz coated on both sides with gold (5 mm in diameter, area $\approx$ 0.2 cm^2, thickness determined by the 9MHz frequency and inferior to 1μm). This piezoelectric element was fixed on a Teflon holder and one of its faces (in contact with the electrolytic solution) was connected both to the oscillator circuit and to the potentiostat. The resonance frequency and the admittance shift of the quartz were measured with a Seiko EGG Model QCA 917 counter. Working electrodes were coated with 30 μg of zinc, thickness 0.2 μm. This coating was obtained by galvanostatic deposition from an aqueous solution of $ZnCl_2$ (1.6 M, Acros 98%) and KCl (5.3 M, Acros p.a.) at 57 °C. As long as the zinc and polymer masses are small compared to that of the crystal, the EQCM works under the so-called "rigid conditions".[39] This means that the linear Sauerbrey relation ($\Delta m = -k\Delta F$)[40] can be used to relate the weight change, Δm (in g) to the resonance frequency shift, ΔF (in Hz). To have good control over the growth of the zinc layer that respects the "rigidity conditions", we used an multipulse electrolysis technique consisting of twenty 2 s pulses of 10 mA cm^{-2} instead of a single 40 s 10 mA cm^{-2} pulse. The "rigidity conditions" of the EQCM response were checked by recording the cell admittance. It varies slightly during the formation of the zinc layer, and during the dissolution of Zn with and without salicylate, but is entirely recovered at the end of the zinc or the zinc salicylate deposition. It is important to note that organic deposition never exceeded thicknesses where the rigidity conditions do not apply.

Polypyrrole surface energy $\Delta\omega$ was deduced from the contact angle θ between the film surface and a water droplet by using the Dupre-Young relationship $\Delta\omega = \gamma\ (1 + \cos\ \theta)$, where γ is the water interfacial energy. Contact angles were measured at the ENSCP (Ecole Nationale Supérieure de Chimie de Paris) with a home-built apparatus consisting of a digital camera and a computer.

Table 1. Electrolysis Bath Composition

[NaSac] (M)	0	1.5	1.9	1.95	2
[DISacH] (M)	1	0.5	0.1	0.05	0
pH	6	5.6	5.4	5.2	5

3. Results

3.1. Voltammetric Study. Different electrolyte mixtures of NaSac and DISacH were used in order to investigate new surface effects induced by the DISacH electrolyte on the Zn electrode. The voltammetric curves related to the electropolymerization of 0.5 M pyrrole were compared for five electrolytic mixtures, with a constant 2 M ionic strength (except for DISacH alone, whose solubility limit is about 1 M) (Table 1). Nonstirred (stationary Zn disk electrode) and stirred (rotating Zn disk electrode) solutions were investigated.

3.1.1. Cyclic Voltammetry at a Stationary Zn Disk Electrode. Addition of DISacH in the electrolytic solution gives rise, with respect to the standard solution (2 M NaSac and 0.5 M pyrrole), to a decrease in the oxidation peak intensities between −1.1 and −0.5 V. These intensities, previously correlated with the formation of an insoluble passive zinc salicylate film,[31] appear in this case extremely low, indicating the formation of an efficient passive layer. They are less than 0.4 mA cm^{-2} when [DISacH] $\geq$ 0.1 M (Figure 1a and the Supporting Information) and about 0.7 mA cm^{-2} when [DISacH] = 0.05 M (Figure 1b). They are about ten times lower than for the same oxidation−passivation peaks obtained with the standard electrolyte (Figure 1c). These results argue in favor of the formation of a strong

(27) da Silva, J. E. P.; de Torresi, S. I. C.; Torresi, R. M. *Prog. Org. Coat.* **2007**, (1), 33–39.
(28) de Souza, S. *Surf. Coat. Technol.* **2007**, (16−17), 7574–7581.
(29) Sazou, D.; Kourouzidou, M.; Pavlidou, E. *Electrochim. Acta* **2007**, (13), 4385–4397.
(30) Tsuchiya, S.; Ueda, M.; Ohtsuka, T. *Isij Int.* **2007**, *47* (1), 151–156.
(31) Petitjean, J.; Tanguy, J.; Lacroix, J. C.; Chane-Ching, K. I.; Aeiyach, S.; Delamar, M.; Lacaze, P. C. *J. Electroanal. Chem.* **2005**, *581* (1), 111–121.
(32) Petitjean, J.; Aeiyach, S.; Lacroix, J. C.; Lacaze, P. C. *J. Electroanal. Chem.* **1999**, *478* (1−2), 92–100.
(33) Xu, L. B.; Chen, W.; Mulchandani, A.; Yan, Y. S. *Angew. Chem., Int. Ed.* **2005**, *44* (37), 6009–6012.
(34) Feng, X. J.; Jiang, L. *Adv. Mater.* **2006**, *18* (23), 3063–3078.
(35) Lim, H. S.; Han, J. T.; Kwak, D.; Jin, M. H.; Cho, K. *J. Am. Chem. Soc.* **2006**, *128* (45), 14458–14459.
(36) Liu, T.; Yin, Y. S.; Chen, S. G.; Chang, X. T.; Cheng, S. *Electrochim. Acta* **2007**, *52* (11), 3709–3713.
(37) Zhu, Y.; Zhang, J. C.; Zheng, Y. M.; Huang, Z. B.; Feng, L.; Jiang, L. *Adv. Funct. Mater.* **2006**, *16* (4), 568–574.
(38) Qu, M. N.; Zhang, B. W.; Song, S. Y.; Chen, L.; Zhang, J. Y.; Cao, X. P. *Adv. Funct. Mater.* **2007**, *17* (4), 593–596.
(39) Glidle, A.; Hillman, A. R.; Bruckenstein, S. *J. Electroanal. Chem.* **1991**, *318* (1−2), 411–420.
(40) Sauerbrey, G. *Z. Phys.* **1959**, *155*, 206.
(41) Torresi, R. M.; Córdoba de Torresi, S. I.; Matencio, T.; De Paoli, M.-A. *Synth. Met.* **1995**, *72*, 283–287.

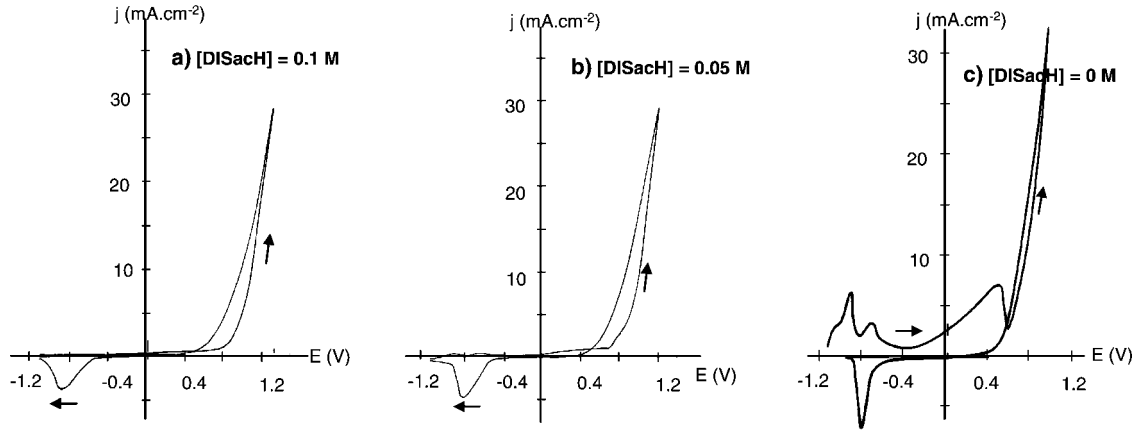

Figure 1. Voltammetric curves obtained on a static Zn disk electrode (diameter 0.5 cm, polished with emery paper 1200 prior to use) at 10 mVs^{-1} in a nonstirred medium. (a) DISacH 0.1 M, NaSac 1.9 M, Py 0.5 M, pH 5.4; (b) DISacH 0.05 M, NaSac 1.95 M, Py 0.5 M, pH 5.2; (c) DISacH 0 M, NaSac 2 M, Py 0.5 M, pH 5. Additional figures are in the Supporting Information.

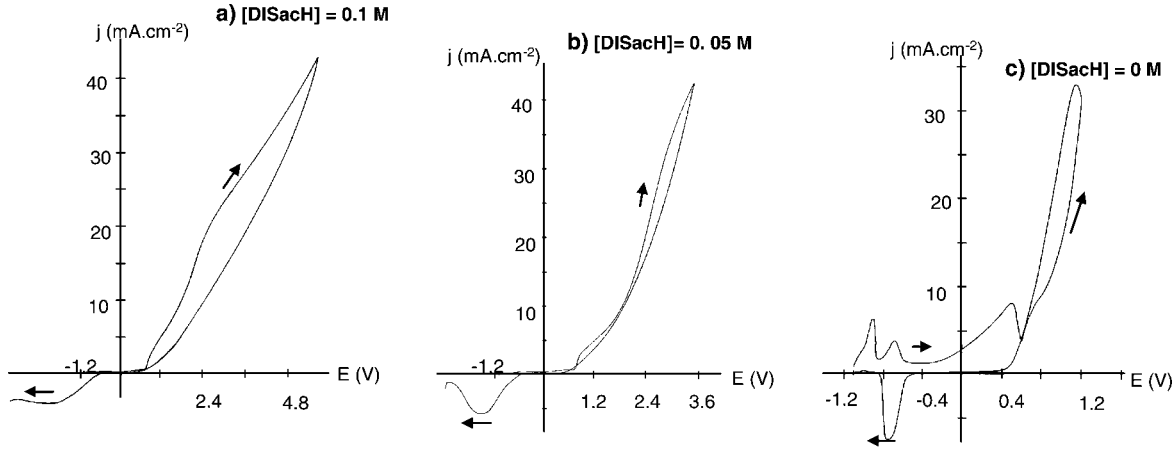

Figure 2. Voltammetric curves obtained on a Zn disk rotating electrode (diameter 0.5 cm, polished with emery paper 1200 prior to use, at 2500 rpm). (a) DISacH 0.1 M, NaSac 1.9 M, Py 0.5 M, pH 5.4; (b) DISacH 0.05 M, NaSac 1.95 M, Py 0.5 M, pH 5.2; (c) DISacH 0 M, NaSac 2 M, Py 0.5 M, pH 5. Additional figures are included in the Supporting Information.

adherent film, more compact, more resistive, and thinner than that obtained with 2 M NaSac alone.

In addition, the presence of the DISacH salt produces an large anodic shift of the pyrrole oxidation wave. Thus, under standard conditions and at 0.8 V, the current density is about 10 mA cm^{-2}, whereas when [DISacH] is over 0.05 M, it decreases to less than 1 mA cm^{-2} (see the Supporting Information for [DISacH] = 0.5 and 1 M).

3.1.2. Cyclic Voltammetry at a Rotating Zn Disk Electrode. Surprisingly, compared to the stationary solution, rotation of the zinc disk electrode (2500 rpm) decreases the current density of the anodic wave corresponding to the oxidation of pyrrole (panels a and b in Figure 2). Thus, the current density at 1.2 V with a solution containing 0.5 M pyrrole and 0.1 M DISacH + 1.9 M NaSac is about 20 mA cm^{-2} in the case of a stationary solution (Figure 1a) and only about 4 mA cm^{-2} when the electrode is rotated (Figure 2a). This unexpected result seems to indicate that the DISacH concentration near the electrode surface is significantly higher than that of NaSac, which in all cases remains fairly constant because of its high concentration, whether the electrode is rotating or not. A possible explanation of this effect is that $Zn(DISac)_2$ is more efficiently precipitated on the zinc electrode than $Zn(Sac)_2$. When the electrode does not rotate, DISacH is depleted near the surface, resulting from formation of the $Zn(DISac)_2$salt and its rapid adsorption on the surface. There is thus a decrease in the DISacH concentration near the surface that is poorly compensated by diffusion in the case of a nonstirred solution. As a consequence, the passivating layer consists mainly of $Zn(Sac)_2$. On the contrary, when the electrode is rotating, mass transport of DISAcH from the bulk toward the surface is more rapid, thanks to convection, and the concentration of DISAcH near the surface remains high and favors the formation of the $Zn(DISAc)_2$ precipitate instead of $Zn(Sac)_2$.

In contrast to sodium salicylate (NaSac), for which similar voltammetric polarization curves were observed under static or stirred conditions (use of a rotating or a nonrotating disk as the working electrode to deposit PPy), in both cases the presence of 3,5-diisopropylsalicylic acid (DISacH) in the electropolymerization medium produces drastic changes in the voltammetric curves. These preliminary observations obviously indicate that the surface phenomena produced at the zinc electrode by the DISacH electrolyte differ markedly from those induced by NaSac.

It is worth noting that the cathodic shift of the polymer reduction peak is also more pronounced when the electrode is

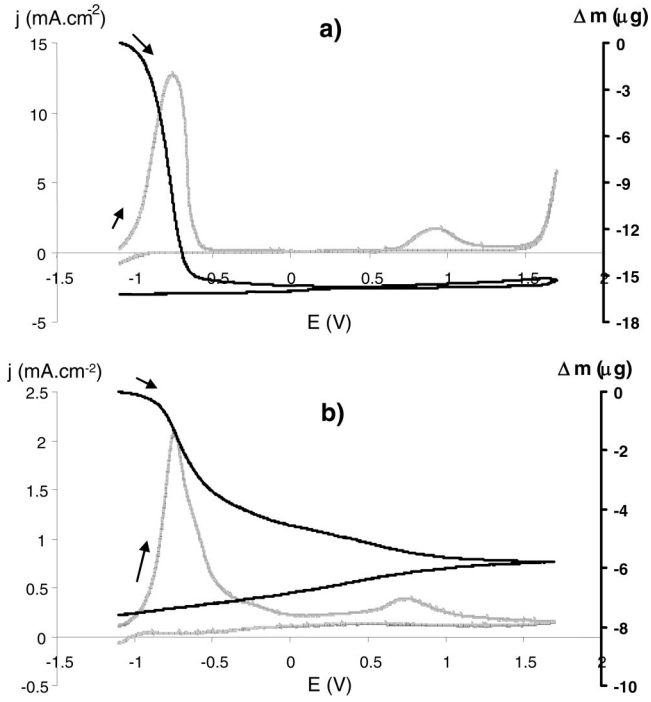

Figure 3. Current density and weight loss curves of a zinc thin layer electrode polarized (forward and backward) between −1 and +1.5 V at 10mV s^{-1}in (a) 2 M NaSac, (pH 5) and (b) 1 M DiSacH, (pH 6).

rotating. Thus, in the case of 0.05 M DISacH + 1.95 M NaSac, the reduction peak is centered at about −0.8 V in a nonstirred solution (Figure 1b) and at −1.5 V when it is stirred (Figure 2b). Moreover, the width of the peak at half-height is about 0.8 V in the first case and about 1.2 V in the latter.

These first results confirm a preferential formation of a zinc−DISacH precipitate with more efficient passivating properties than those obtained with sodium salicylate alone.

3.2. Measurements with a Quartz Crystal Microbalance. These experiments were carried out to compare the passivation steps related to NaSac and DISacH and to examine how the anions behave during the dedoping of the polymer.

3.2.1. Passivation of the Zinc Layer in the Presence of DiSacH. The gold-coated quartz plate was first covered with a zinc layer 0.2−0.3 μm thick, as described in the experimental part (this thickness corresponds to approximately 150 μg cm^{-2} of zinc). When NaSac alone is used as the supporting electrolyte, almost half the zinc layer is wiped out during the first voltammogam cycle (Figure 3a). On the contrary, when DISacH is used, a weight loss of only about 5 μg is observed during the first sweep, i.e., three times less than with NaSac (Figure 3b). As a consequence, when the potential reaches that of pyrrole oxidation, the gold layer remains almost completely covered by the Zn layer. Therefore, the electrochemical results concern zinc, even though the active layer may have electrochemical properties that could slightly differ from those of bulk zinc. In particular, we note that the peak intensities corresponding to zinc passivation by DiSacH (Figure 3b) are much higher than those of Figure 1 obtained on bulky zinc.

The weight of the passive layer is a function of the applied potential and can be calculated from the difference between the theoretical weight loss curve m_{th} (it is assumed that Zn

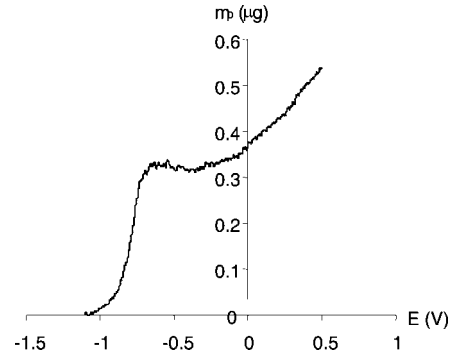

Figure 4. Variation of the weight of the passive layer $m_p = m_{th} - m_e$ versus the applied potential.

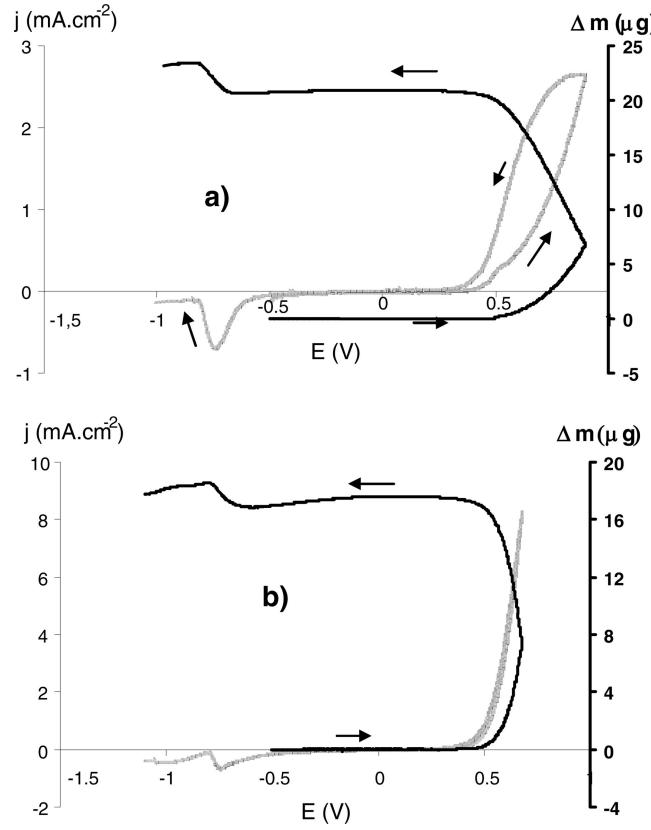

Figure 5. Voltammetric curves and weight variation recorded during PPy formation at gold electrode in (a) 1 M DISacH+ 0.5 M Py at pH 6 and (b) 2 M NaSac +0.5 M Py at pH 5.

dissolution gives Zn^{2+}) and the experimental weight loss curve m_e for the first voltammetric sweep (figure S3 displays m_{th} and m_e versus versus the faradaïc charge corresponding to the zinc oxidation $Q(C)$). The results reported in Figure 4 show a first rapid weight increase from −1 V to −0.7 V followed by a plateau at 0.35 μg from −0.7 to −0.2 V corresponding to the formation of a passive layer below 8 nm thickness (assuming a mean density of 2 for the $Zn(DISac)_2$complex). A slight weight increase up to 0.5 V occurs, corresponding to a slower growth of this passive layer.

From these results, it appears that the presence of DiSacH in the solution generates a passive layer on the zinc electrode which is much thinner than that formed in NaSac medium (about 15 nm as previously determined) and that is obtained with much less zinc dissolution. Despite the fact that the passivation layer thickness is on the order of a few nanom-

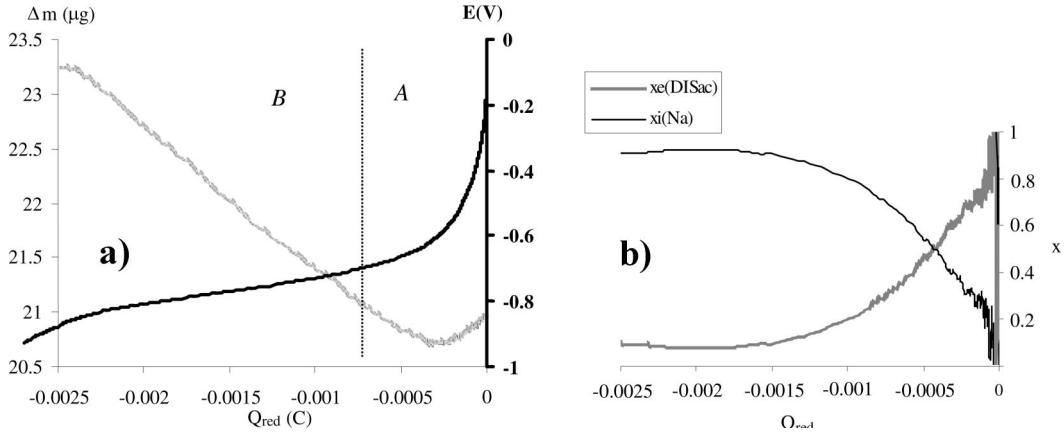

Figure 6. (a) Relation between the potential E of the gold coated quartz cristal electrode with the reduction charge Q_{eed} and variation of Δm with E and Q_{red}. (b) Variation of x_e and $x_i = 1 - x_e$ with Q_{red} calculated from eq 4.

eters, it remains sufficiently compact to impede zinc oxidation without preventing pyrrole oxidation.

3.2.2. PPy Doping and Dedoping with DISacH. These measurements were carried out on a gold-coated quartz crystal electrode in order to exclude all weight variations due to zinc dissolution and passivation, and compared to the 2 M NaSac standard medium with 0.5 M pyrrole. Although the concentrations of the two electrolytes are different (2 M NaSac and 1 M DISacH), this is of no electrochemical importance in the case of a gold electrode.

The curves of Figure 5a are similar to those obtained in the presence of salicylate (Figure 5b), with a first weight increase starting in both oxidation cases at about 0.5 V, corresponding to PPy film formation, and followed in reduction by a second fast weight increase corresponding to cation insertion at about −0.70 V with NaSac and at about −0.75 V with DISacH. However, a significant difference appears between the two systems. In the case of NaSac and from 0 V up to −0.7 V, a slow weight decrease occurs that corresponds to anion expelling from the film. This does not occur with DISacH, a fact that indicates that the bulky anion remains entrapped in the film during the reduction process and that charge compensation occurs mainly through Na^+ insertion. Putting Q_{ox} as the anodic charge corresponding to pyrrole oxidation, M_{Py} and M_D the molecular weights of pyrrole and doping anion, respectively, y the doping yield of PPy (0.22), and F the Faraday constant, the theoretical PPy weight (m_{PPy}^{theor})deposited on the surface is then given by eq 1.

$$m_{PPy}^{theor} = \frac{Q_{ox}}{F}\frac{M_{Py} + yM_D - 2}{2 + y} \quad (1)$$

Similarly, the theoretical charge Q_{red}^{theor} for the complete reduction of the doped PPy is deduced from eq 2.

$$Q_{red}^{theo} = \frac{y}{2 + y}Q_{ox} \quad (2)$$

We assume that the reduction step might result from two different mechanisms: either the doping anion is totally expelled from the film, and in this case, the weight loss Δm_e is given by the relation $\Delta m_e = (Q_{red}/F)M_{D,}$or the doping anion remains entrapped in the film, and charge compensation occurs through cation insertion (Na^+). In this latter case, there is a weight increase Δm_i given by the relation $\Delta m_i = -(Q_{red}/F)(M_C + hM_W)$, where M_C and M_W are the molecular weights of the cation and water, respectively, and h the number of water molecules that constitute the cation solvation layer (h was reported to be 4.5 in the case of NaCl).[41]

If we consider that both mechanisms occur simultaneously, and with x_e and x_i the percentages of the reduction charge for a given applied potential, due to anion expulsion or cation insertion, respectively, the experimental weight variation Δm is given by eq 3.

$$\Delta m = x_e\Delta m_e + (1 - x_e)\Delta x_i \quad (3)$$

From eqs 13, x_e is deduced, according to eq 4.

$$x_e = \frac{1}{M_D + M_C + hM_{H2O}}\left(M_C + hM_{H2O} + \frac{F\Delta m}{Q_{red}}\right) \quad (4)$$

We report in Figure 6a the variation of the potential and the weight variation of a PPy film doped with DISacH versus the reduction charge Q_{red}, in which we can distinguish two regions noted A and B corresponding to two different variations of Δm with Q_{red}. From −0.75 mC up to −2.5 mC (region B) the variation of Δm is positive and linear with Q_{Red} with a slope of about 1.3×10^{-3} g C^{-1}, very close to the theoretical slope (1.1×10^{-3} g C^{1-}) for cation insertion (Na^+ and 4.5 H_2O). This result shows that the reduction at potentials lower than −0.7 V is associated with cation insertion, and not with anion loss. Dedoping region between 0 and −0.7 V, noted A, is mixed with cation insertion and concerns a very low charge fraction of about −0.75 mC. This behavior differs markedly from that of a standard PPy film doped with NaSac, for which exclusion of the doping anion appears to be the main process (59% of the reduction charge). On the contrary, with the $DISac^-$ anion, the cation insertion mechanism is very important as is confirmed by the x_e value which is about 90% at the end of reduction (Figure 6b).

In conclusion, the mobility of $DISac^-$ in PPy is lower than that of Sac^-; it will make the reduction of the doped polymer more difficult, and therefore, this should lead to an improvement in the protection properties against corrosion.

3.3. Electrochemical Characterization of PPy Films Synthesized in Galvanostatic Mode in the Presence of DiSacH. *3.3.1. PPy Film Formation at Low Current Density:* j = *10 mA cm* $^{-2}$ *for 1 min* (Q = *0.6 C cm*$^{-2}$.).

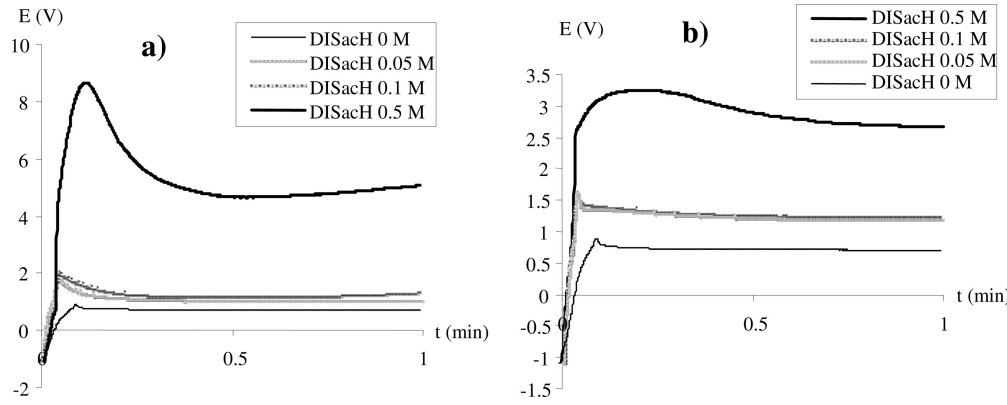

Figure 7. Chronopotentiometric curves $E = f(t)$ obtained on a zinc disk electrode (diameter 1 cm), for an applied current density $j = 10$ mA cm^{-2}. Salt mixtures and electrolyte conditions are the same as in Figure 1. (a) Nonrotating electrode; (b) rotating electrode (2500 rpm).

When oxidation of 0.5 M pyrrole is carried out in a nonstirred 1 M DISacH solution, homogeneous film formation does not occur and in all the cases the potentiostat is saturated (the potential rises to over 12 V). Such behavior is not very surprising, and this confirms the strong insulating character of the passive layer, formed prior to electropolymerization, which could also be predicted from the large anodic shift of the pyrrole oxidation wave observed on voltammetric curves (see Figure S1 in the Supporting Information).

In the case of NaSac/DISacH mixtures and in the absence of stirring (Figure 7a), PPy films can be electrodeposited. For 0.5 M DISacH + 1.5 M NaSac the chronopotentiometric curve passes through a potential peak (around 8.5 V), which can yet be attributed to the high resistance of the native passive layer. About 10 s later, the potential decreases slowly, to 5 V, which is probably due to a structural rearrangement of this layer caused by an interpenetration of conductive PPy paths inside the passivating layer. After this first decrease, the potential slowly increases again, and at the same time, a slight salt deposit is observed resulting from the precipitation of DiSacH, caused by a local increase in the acidity resulting from pyrrole polymerization.

For DiSacH concentrations below 0.5 M, the characteristics of the chronopotentiometric curves change dramatically. For 0.1 and 0.05 M DiSacH, the chronopotentiometric curves are very similar: the peak potential is now very flat and the potential remains stable throughout the electrolysis. Only a very slight overvoltage (about 0.2 V) with respect to the chronopotentiometric curve of Na Sac alone is observed.

Again, marked changes in the chronopotentiometric curves occur when the electrode is rotating ($\omega = 2500$ rpm) (Figure **7**b), and obviously this is caused by a modification of the structure of the passive layer. The first point to be mentioned is the lower overvoltage reached by the electrode during electropolymerization, indicating a lower resistance of the passive layer. In the case of 0.5 M DiSacH, the potential maximum is only 3.2 V instead of 8.5 V in the case of the stationary electrode, a result that can be interpreted as a decrease of about 500 Ω cm^{-2} in the resistance of the passive layer. Such a result must be attributed to the fact that interpenetration of PPy paths is easier when the electrode is rotating than when it is immobile. This hypothesis is also confirmed by the fact

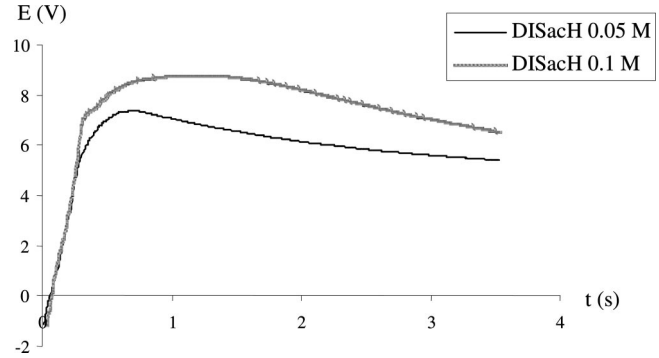

Figure 8. Chronopotentiometric curves $E = f(t)$ obtained on a rotating (2500 rpm) zinc disk electrode at $j = 200$ mA cm^{-2} and under the same conditions as those of Figure 7b.

that the initial peak is dramatically flattened and that the potential is better stabilized in the case of high DiSacH concentrations. The effect is less pronounced at the lowest DiSacH concentrations; however, the difference compared to NaSac alone remains significant, and an overvoltage of about 0.6 V with respect to the NaSac curve is observed, corresponding to an increase of about 60 Ω cm^{-2} in the resistance of the passive layer.

Rotation of the electrode has a further advantage in that it impedes the precipitation of the salt on the film. Film analysis by SEM showed that the morphology of the coatings is similar to that of standard films obtained with NaSac alone and that the thickness after 1 mn of synthesis is close to the theoretical value of 2 μm.

3.3.2. High Current Density: j = *200 mA cm^{-2} for 3.5 s.* In the case of high DiSacH concentrations ([DISacH] = 0.5 M), either with or without stirring, PPy film deposition is impossible, because it entails the saturation of the potentiostat.

For [DISacH] ranging between 0.05 M and 0.1 M (Figure 8), the potentials at which PPy is formed are 6 and 7 V, respectively, at the end of the deposit, much higher than that observed for the standard solution (4 V). In all cases, the films (2 μm thick) are homogeneous and have a morphology identical to that observed for standard films of the same thickness. Moreover, in spite of the high value of the current, rotation avoids the precipitation of DiSacH on the film, a result that is particularly important for obtaining good protection properties against corrosion and is compatible with

application to an industrial process, such as the coil coating, which requires fast deposition. In the following, these conditions will be called "industrial conditions".

3.3.3. Determination of the Film Doping Ratios between NaSac and DiSacH for Various Concentrations of NaSac and DISacH. The fact that a small addition of DiSacH in the medium considerably modifies the polarization curves observed during the PPy deposition is quite intriguing. The whole doping yield (DiSacH + SacH), measured from the N1s XPS signal, is about 22% and remains fairly constant for all DiSacH/SacH ratios and, furthermore, is identical to that of a standard film obtained with NaSac alone.

Preferential doping by DiSacH is probably the cause of this behavior. Unfortunately, for the determination of these ratios, XPS, which is particularly well-suited for a quantitative analysis of a single dopant in the film, is here unhelpful and a chemical procedure is necessary. Best results were obtained following the chemical procedure described below: (i) reduction of PPy films by immersion of the samples for 48 h in an 0.1% aqueous NaOH solution; (ii) recovery of the doping agents in the form of acids after acidification of the aqueous phase by HCl (to pH 1) and extraction with ether; (iii) determination of the DiSacH/SacH ratio by gas chromatography coupled to a mass spectrometer (GC-MS). Chemical ionization was selected because it prevents the fragmentation of the molecules and favors the formation of the molecular ion and, therefore, facilitates its quantitative determination.

It should be stressed that this method assumes that the totality of the 3,5-diisopropylsalicylate is expelled during the reduction step in basic solution, despite the quartz microbalance results, which indicate low mobility of the doping agent in the coating. Preliminary tests carried out on zinc plates covered with standard polypyrrole confirmed that the totality of salicylate present in films was recovered by this technique. Thus, in the case of a salicylate and diisopropylsalicylate codoping, partial recovery of this latter salt would involve a decrease in the whole doping yield.

SacH/DISacH mixtures were made in acetonitrile with a total concentration of 10 mg mL^{-1}. With n(SacH)/n′(DISacH) ratios of 0.3, 1, and 3 (n and n' representing the numbers of moles of each acid), and applying the procedure described previously, we found a linear relationship between the true ratio of the two acids (R_t) and the experimental ratio measured by mass spectrometry (R_{ms}) corresponding to $R_{ms} = 0.8R_t$ (see the Supporting Information, Figure S4). This relationship is valid as long as the total concentration exceeds 1 mg mL^{-1}.

Putting y the rate of total doping of PPy films, y_{Sac} and y_{DISac} the rates of partial dopings by salicylate and 3,5-diisopropylsalicylate, respectively, we calculate y_{Sac} and y_{DISac} from the two relations below

$$\begin{cases} y = y_{sac} + y_{DISac} \\ \dfrac{y_{Sac}}{y_{DISac}} = R_t \end{cases} \quad (5)$$

The values listed in Table 2 show there is preferential doping of PPy films by $DISac^-$. Indeed, a small concentration of DISacH in the bath can lead to a high concentration of this salt in the PPy film. The fact that the $DISac^-$ concentration in the film is about 10 times greater than its concentration in the solution is quite surprising and seems to be specific to this salt.

Table 2. Partial Doping Yields of Ppy Films Obtained under "Industrial Conditions"

solution composition			PPy			
[NaSac] (M)	[DISacH] (M)	% DISacH	y	y_{Sac}	y_{DISac}	% $DISac^-$
2	0	0	0.22	0.22	0	0
1.95	0.05	2.5	0.22	0.16	0.06	29
1.9	0.1	5	0.22	0.08	0.14	62

Table 3. Evolution of the Contact angle with the DISacH Concentration; Young Dupre Relationship ($\Delta\omega = \gamma(1 + \cos\theta)$ was Used to Calculate the Surface Energy, $\Delta\omega$

	[DISacH] (M)		
	0	0.05	0.1
θ	100	115	125
$\Delta\omega$ (mJ m^{-2})	59.8	41.8	30.9

Such an effect of preferential doping is not generalizable to other electrolyte mixtures. Indeed, we found that, all other things being equal (0.5 M Py, pH 6), in the case of 2 M NaSac +0.5 M *p*-toluenesulfonic acid (i.e., 25% of *p*-toluenesulfonic acid with respect to the total electrolyte concentration), only 7−10% of the doping anion was ascribable to the coelectrolyte.

3.3.4. Characterization of PPy Films Synthesized in the Presence of Disach under "Industrial Conditions". Independently of the DISacH concentrations in the solution (0.1 or 0.05 M), the resistance of the polymers, measured in a dry state, remains fairly constant around $R = 10\ \Omega$, from which we deduce a specific conductivity $\sigma = 1 \times 10^{-4}$ S cm^{-1}, three times less than that of the standard PPy film.

The introduction of DISacH into the film leads also to a decrease in the energy of the surface, which becomes more hydrophobic. This was deduced from the measurement of the contact angle θ resulting from the contact of a water droplet with the PPy film (Table 3).

It should be stressed that the angles measured for [DISacH]>0.05 M are very high and higher than those reported in the literature for aliphatic insulating polymers (θ between 95 and 107° in the case of polyethylene) or fluorinated polymers ($\theta \approx 112-117°$ for Teflon). Beyond an increase in the hydrophobicity of the coatings with the DISacH concentration, such an evolution of θ could be due to an increase of surface roughness, as occurs with superhydrophobic surfaces. [33–38] However, an MEB analysis of the surface did not show any significant morphology difference between a film containing DISacH and a standard film without DISacH.

This evolution of the surface energy presents two major interests:

(i) an increase in the hydrophobicity of the coating would improve the barrier effect toward water and therefore improve the anticorrosion properties;

(ii) if PPy film is to be used as a primer, control of the surface energy makes it possible to optimize the interaction with a top coating.

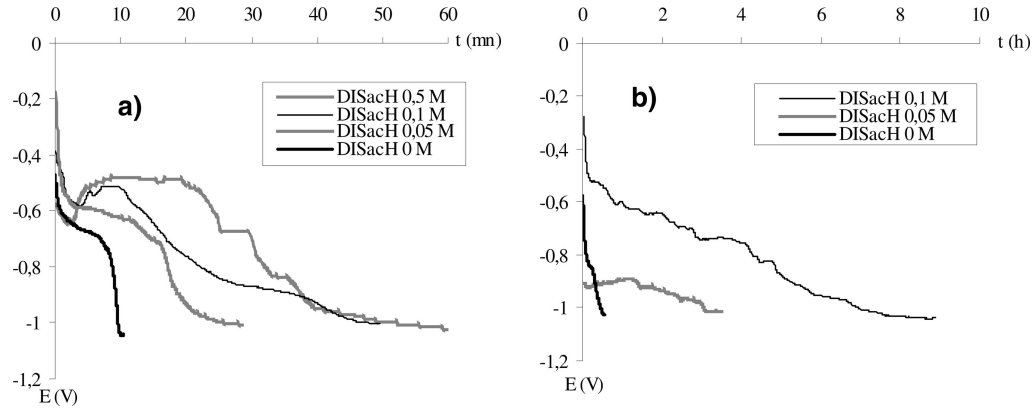

Figure 9. Open circuit potential curves $E-t$ of a 2 μm thick PPy film coated zinc electrode immersed in a 3.5% NaCl solution. The PPy films were obtained at a rotating electrode (2500 rpm) with a constant total DISacH + NaSac concentration equal to 2 M, and with DISacH concentrations ranging from 0 to 0.5 M. (a) Film synthesis was carried out under normal conditions: 10 mA cm^{-2} for 1 min. (b) Film synthesis carried out under "industrial conditions": 200 mA cm^{-2} for 3.5 s.

Table 4. Coefficients of Protection P_{10} and P_{200} Obtained with Various DISacH + NaSac Mixtures at a Total Concentration of 2 M

	[DISacH] (M)			
	0	0.05	0.1	0.5
P_{10}	1	2.5	5	5
P_{200}	1	6	16	

Furthermore, an increase in zinc roughness or a nanostructuration of the underlying metal is likely to yield superhydrophobic and smart surfaces with reversibly switchable wettability. Future work in this area will be reported elsewhere.

3.3.5. Evaluation of Protection against Corrosion with Native Films. A PPy-coated zinc electrode (2 μm thick), obtained with various DISacH concentrations under normal (10 mA cm^{-2}, 1 min) or "industrial conditions" (200 mA cm^{-2}, 3.5 s) was immersed in a 3% NaCl solution. The anticorrosion properties were evaluated in two ways: the open-circuit potential of the electrode and the Zn^{2+} concentration were recorded as a function of time.

In comparison with sodium salicylate alone, the open-circuit potential curves of Figure 9 clearly show that addition of DISacH in the electrolytic bath improves the protection properties of the film. The time necessary to return to the zinc corrosion potential of about −1 V is much longer when the film is synthesized with DISacH. Moreover, in the case of PPy synthesized under "industrial conditions" the time of return to this corrosion potential is about a couple of hours while for PPy synthesized at 10 mA cm^{-2} it is less than an hour. This property is estimated more quantitatively as a coefficient of protection P, which allows a direct comparison of standard and modified PPy films. Thus, P is defined as the ratio of the "return times" for PPy films prepared with DISacH + NaSac and with NaSac alone.

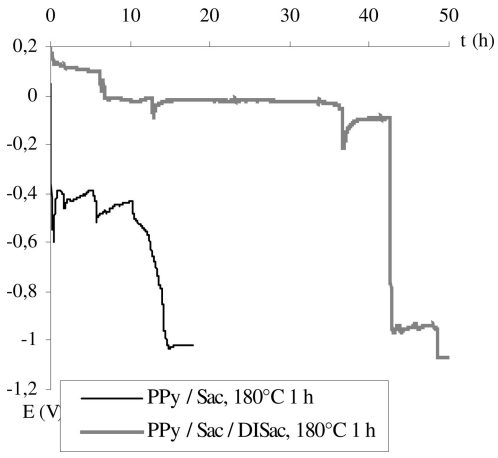

Figure 10. Open-circuit potential−time curves of cured coated PPy zinc electrodes in a 3.5% NaCl solution.of PPy−zinc electrodes cured in air for 1 h at 180 °C; PPy films synthesized in 2 M NaSac + 0.5 M Py at pH 5 and 1.9 M NaSac + 0.1 M DISacH + 0.5 M Py at pH 5.4.

P_{10} and P_{200} are the corresponding P values for PPy films synthesized at 10 and 200 mA cm^{-2}, respectively. The P values reported in Table 4 show that the best results are obtained for PPy films synthesized under "industrial conditions".

Nevertheless, these values are not good enough for these coatings to be used for corrosion protection. In spite of their good hydrophobic properties, the coatings remain highly permeable to water, probably because the water content is high because the films are prepared in aqueous medium. To check this point, we have carried out the thermal analysis of the films and tested their protection properties.

3.3.6. Evaluation of the Protection Properties of PPy-Coated Zinc after Heat Treatment. Thermal aging of conducting polymers has already been described and results generally in a thermal-oxidative degradation consisting in the loss of conductivity and electroactivity. If the temperature is held below 180 °C, under N_2 or air, the PPy polymer and its doping salt remain stable, but all the water inside the film is evaporated. DTA-TGA (differential thermal analysis−thermal gravimetric analysis) show that the water content is about 2% in the case of PPy films synthesized with 0.1 M DISacH + 1.9 M NaSac and 6% with 2 M NaSac, in agreement with the fact that hydrophobicity of PPy films increases from NaSac to mixtures of DISacH + NaSac. Above 180 °C, and particularily in air, a greater weight loss is observed, attributed to an exothermal reaction with oxygen leading to PPy cross-linking.

On account of these observations, heat treatment at 180 °C for an hour was applied to PPy films in air, and their

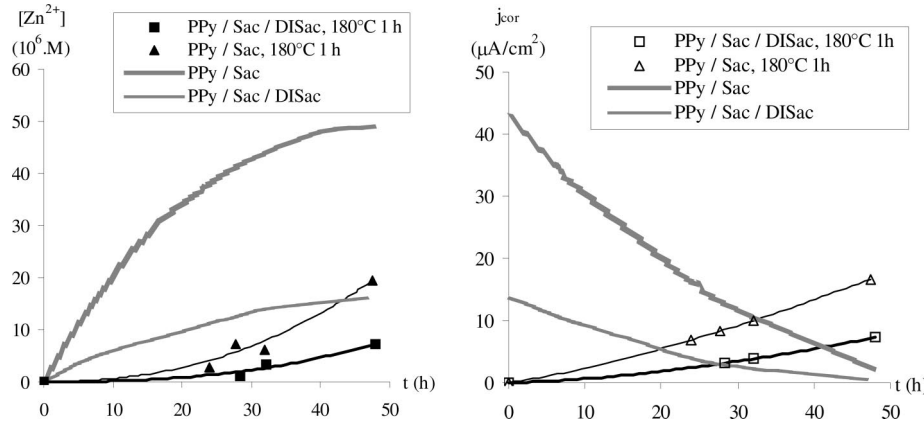

Figure 11. Corrosion curves of PPy-coated zinc electrodes immersed in a 3.5%NaCl solution. The PPy films were synthesized as previously under "industrial conditions". Comparison is made between air cured (180 °C, 1 h) and native films. Evolution of the a) Zn^{2+}concentration with time. b) corrosion current density with time.

protection properties were then tested by two methods. The first technique used was that of the time dependence of the electrode potential in a 3.5% NaCl solution. The second, based on the corrosion current density measurement, consisted in determining versus time the Zn^{2+} concentration resulting from the corrosion of the coated electrode immersed in the same solution.

(i) Estimation of the protection properties of cured films by the method of the electrode potential time dependence. As previously, the films were synthesized under industrial conditions, either in presence of 2 M NaSac alone or in presence of 1.9 M NaSac + 0.1 M DISacH. In both cases, the curing process leads to important improvements, as is attested by the shift of the corrosion potential toward more anodic potentials, but also by an increase in the P_{200} value.

The time-dependence electrode potential curves (Figure 10) clearly show these improvements, more still pronounced in the case of films synthesized with DISacH. In the case of NaSac alone, the corrosion potential lies between −0.4 and −0.6 V for 10 h and then drops abruptly until the zinc metal corrosion potential at about −1 V, which corresponds to a P_{200} value of about 16, in comparison to the P_{200} value of 1 for the same native coating. With PPy films synthesized with DISacH the corrosion potential remains between 0.2 and 0 V, and goes back to the zinc corrosion potential at −1 V after more than 30−40 h, corresponding to a P_{200} value of 100.

However, it must be noted, that in contrast to native films, the return to the zinc metal corrosion potential is more abrupt. This could be indicative of defects occurring in the film during its immersion in the NaCl solution. Besides, the protection properties seem to be strictly correlated with the presence of O_2 during the curing step. The same curing step carried out in presence of N_2 does not improve the protection properties as much (see Figure S5 in the Supporting Information). The corrosion potential decreases rapidly from −0.6 to −1 V in less than half an hour in the case of films synthesized with DISacH, and no significant difference appears with cured NaSac films compared to native films synthesized under the same conditions.

(ii) Determination of the corrosion current density. As previously, the coated zinc electrode was immersed in a 3.5% NaCl solution. Sampling of the solution was carried out versus time and the Zn^{2+} concentration was measured by polarography. The samples removed from the solution were small in order not to disturb the initial concentration by more than 1−2%.

Putting V, the volume of solution in which is immersed the zinc electrode, S, the surface area of the coated zinc electrode in contact with the corrosive bath, and $[Zn^{2+}]$ the concentration of zinc ions resulting from the dissolution of Zn, then the corrosion current density j_{cor} can be deduced from eq 5

$$j_{cor} = \frac{2VF}{S}\frac{d[Zn^{2+}]}{dt} \quad (6)$$

The curves of Figure 11 recorded for a period of about 50 h show there is a considerable improvement in the protection properties, due to an increase in the barrier effect of the polymer. Thus, with respect to a bare zinc electrode, the corrosion current density at time 0 is about 820 times lower for cured PPy films synthesized in the presence of NaSac, and 8200 times lower for cured films prepared with 0.1 M DISacH + 1.9 M NaSac. In the case of cured films the corrosion current density increases slowly with time; on the contrary, it decreases with noncured films. This may be explained by the fact that in the case of noncured films, the marked corrosion at the beginning of the experiment leads to the formation of blisters and to partial detachment of the film, which favor precipitation of insulating zinc hydroxides, and therefore the decrease in j_{cor}.

4. Conclusion

The use of DISacH as a coelectrolyte has led to several improvements in PPy films obtained under "industrial conditions". In spite of an increase in the film resistivity it is nevertheless possible to deposit on the zinc surface a PPy film 2 μm thick in an extremely short electrolysis time, corresponding to applying 200 mA cm^{-2} for 3.5 s. The preferential doping of PPy by the 3,5-diisopropylsalicylate anion induces drastic changes in the properties, not only for the formation of the passive layer but also of the PPy film.

Among several effects due to the presence of DISac, the most important are a significant increase in surface hydrophobicity and an increase in the barrier effect, particularly high after the films have been cured at 180 °C for an hour in air. This treatment is more than a dehydration process and corresponds to a deep structural modification, probably a cross-linking reaction, which will be the subject of a future study.

Acknowledgment. The authors thank SOLLAC for financial support of this work.

Supporting Information Available: Additional figures (PDF). This material is available free of charge via the Internet at http://pubs.acs.org.

CM703658T